A BIDIRECTIONAL KNUDSEN PUMP WITH SUPERIOR THERMAL MANAGEMENT FOR MICRO-GAS CHROMATOGRAPHY APPLICATIONS

Qisen Cheng[1,3], Yutao Qin[1,2], and Yogesh B. Gianchandani[1,2,3]
[1]Center for Wireless Integrated MicroSensing and Systems (WIMS[2])
[2]EECS Department, [3]Department of Mechanical Engineering
University of Michigan, Ann Arbor, Michigan, USA

ABSTRACT

Bidirectional gas flow is needed for many microsystems, in particular gas chromatographs. This paper reports a bidirectional Knudsen pump (KP) with superior thermal management. Without moving parts, the KP is reliable, silent, and scalable. However, a bidirectional KP requires controlled heat dissipation that matches the pumping need in each direction. This work integrates a micromachined KP chip that has an effective pumping area of 16×16 mm^2, with two customized planar heat sinks with prescribed heat dissipation. This KP produces a maximum air flow rate of ≈0.82 sccm and a maximum blocking pressure of ≈880 Pa at 2 W. The overall bidirectional performance is improved by 2X-3X compared to prior work, as a consequence of effective thermal management.

INTRODUCTION

Bidirectional gas flow is essential for many microsystems. Examples include valve manifolds for liquid phase microanalytical systems [1]; vapor sampling elements for mass spectrometers [2] and gas chromatographs [3]; and pressure-controlled environments for manufacturing and other applications. In most cases, gas flow is routed through multiple valves to permit the reversal of flow direction. The requirement of valves increases system complexity, cost, and failure rates. Bidirectional gas pumps can eliminate these concerns for certain microsystems [4-5].

Knudsen pumps (KPs) have been reported as promising candidates for bidirectional pumping [4-5]. KPs operate on the principle of thermal transpiration [6]: within channels that restrict the flow of gas molecules to non-viscous flow regimes, the net flux in the absence of a pressure differential is against the temperature gradient, *i.e.* from the cold side to the warm side. Compared to motion-based pumps, KPs avoid friction losses, stiction, and noise generation problems. Therefore, KPs are highly reliable, silent, and scalable.

In a typical implementation of high-flow unidirectional KPs, nanoporous membranes provide numerous parallel channels between a Joule heater and a heat sink [7]. The low thermal conductivity of the membranes allows a large temperature gradient to be established across the membranes. Bidirectional KPs have been implemented by either integrating thermoelectric elements [8] or attaching Joule heaters and heat sinks on both sides of the nanoporous membranes [4-5]. The flow direction can be switched by simply changing the current directions for the former approach or powering different Joule heaters for the latter approach.

A major challenge for designing a bidirectional KP is the contradictory requirements for heat sinks that depend upon the flow direction. For example, a large heat sink benefits performance when it is located on the cool upstream side, but greatly diminishes performance when flow is reversed. At a given power level, achieving a large temperature difference between the hot and cold sides of the KP with a low average temperature would improve the overall performance. Using Sharipov's equation [9] for a single flow channel:

$$\dot{M}_{TT} = \left(\frac{Q_T \Delta T}{T_{avg}} - \frac{Q_P \Delta P}{P_{avg}}\right) \frac{\pi a^3 P_{avg}}{l} \left(\frac{m}{2k_B T_{avg}}\right)^{0.5} \quad (1)$$

where $\dot{M}_{TT}$ is the standard mass flow rate through a single channel; a is the hydraulic radius of the channel; l is the channel length; m is the mass of the gas molecules; k_B is the Boltzmann constant; Q_T is thermal creep flow coefficient; Q_P is the viscous flow coefficient; ΔT is the temperature difference between two channel ends; ΔP is the pressure difference between two channel ends; T_{avg} is the average temperature; P_{avg} is the average pressure. Ideally, ΔT should be large and T_{avg} should be modest.

This paper presents a bidirectional KP that integrates a micromachined KP chip with two customized heat sinks that provide asymmetrical flow that is tailored for the operation of a micro-gas chromatograph (μGC). The structure is intended to be simple to manufacture and assemble.

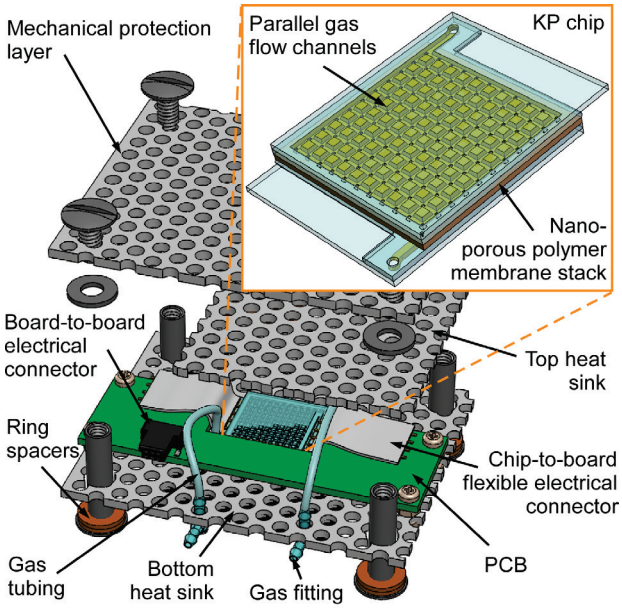

Figure 1: 3D model of Knudsen pump with a zoom-in of the KP chip assembled inside. A stack of five membranes is sandwiched between micromachined glass dies.

DESIGN AND MODELING

Design and Analysis

The proposed structure sandwiches a micromachined KP chip between two unequally sized perforated planer metal heat sinks (Fig. 1). The KP chip consists of a stack of mixed cellulose ester (MCE) membranes (Millipore, MA, USA) sandwiched between glass dies with micromachined gas flow channels and thin-film metal (Ti/Pt 25/100 nm) heaters and thermistors (Fig. 2). The effective pumping area of the KP chip is 16×16 mm^2.

The KP chip is sandwiched between two aluminum meshes (McMaster-Carr, OH, USA) that serve as heat sinks. The aluminum meshes are 1.6 mm thick, and are 40% perforated with 3.2 mm diameter holes in a staggered array pattern. The bottom heat sink is also a base for the other components, including a PCB and gas fittings for interfacing external gas tubing. The metal heaters and thermistors embedded in the KP chip are all wired to the PCB which provides electrical connection to external test setup. The inlet and outlet of the KP chip are both connected to tube fittings using flexible gas tubing. The bottom heat sink is elevated by ring spacers from the ground to permit efficient convective cooling. A third mesh located at the top of the KP serves as a mechanical protection layer without compromising convective cooling of the lower heat sinks. The fully assembled KP has a footprint of 60×82.4 mm^2 (Fig. 2). Compared to bulky commercial heat sinks, the thin and planar shape of the customized heat sinks enhances conductive heat spreading from the KP chip. The perforations on the heat sink facilitate natural convection and enlarge the effective convection area.

Modeling

The only source of heat in the arrangement is the KP chip. The heat dissipation from the chip to the ambient can be modeled by an equivalent thermal circuit (Fig. 3). The main components include: the thermal resistances of heat conduction from the heater to the top and bottom heat sink ($R^{cd}{}_1$ and $R^{cd}{}_2$); the thermal resistances of heat spreading in the top and bottom heat sink ($R^{sp}{}_1$ and $R^{sp}{}_2$); and the thermal resistances of heat convection from the top and bottom heat sink to the ambient ($R^{cv}{}_1$ and $R^{cv}{}_2$). The conductive and convective thermal resistances can be approximated as [10]:

$$R^{cd}{}_1 = \frac{t^{die}{}_1}{k_{die} \cdot A_{die}} \quad (2)$$

$$R^{cd}{}_2 = \frac{t^{die}{}_2}{k_{die} \cdot A_{die}} + \frac{t_{MCE}}{k_{MCE} \cdot A_{MCE}} \quad (3)$$

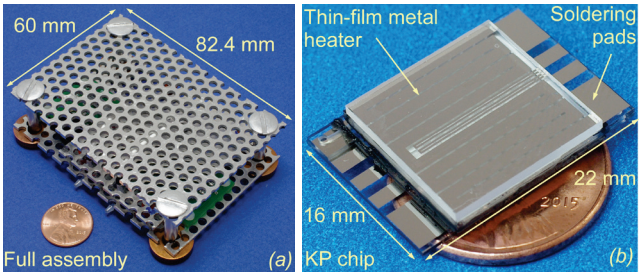

Figure 2: Photos of (a) Knudsen pump (full assembly), and (b) Knudsen pump chip assembled inside.

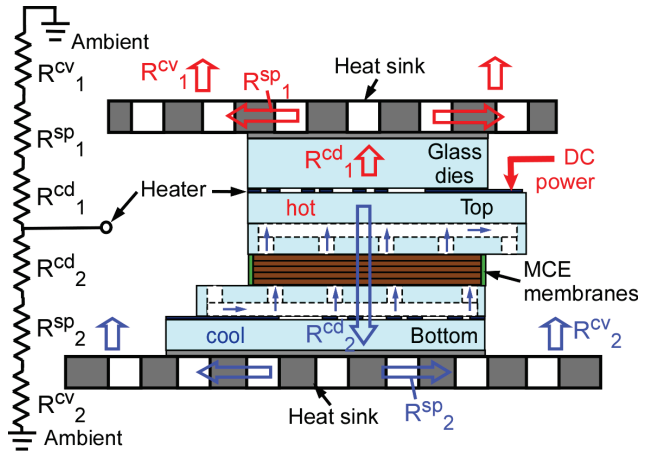

Figure 3: Equivalent thermal circuit of heat dissipation from the KP chip to the ambient.

$$R^{cv}{}_1 = \frac{1}{h^{air} \cdot A^{eff}{}_1} \quad (4) \qquad R^{cv}{}_2 = \frac{1}{h^{air} \cdot A^{eff}{}_2} \quad (5)$$

where t_{MCE} is the thickness of MCE membrane stack, and $t^{die}{}_1$ and $t^{die}{}_2$ are the thicknesses of glass dies above and below the heater, respectively; k_{MCE} and k_{die} represent the thermal conductivity of MCE membranes and glass dies, respectively; A_{MCE} and A_{die} are the footprints of the MCE membrane stack and the KP chip, respectively; $A^{eff}{}_1$ is the effective heat convection area of the top heat sink, and $A^{eff}{}_2$ is that of the bottom heat sink; h^{air} is the heat convection coefficients of air for both top and bottom heat sinks, which can be estimated using thermodynamic theory [10]. The thermal resistances of heat spreading can be estimated using Yovanovich's expression [11]:

$$R^{sp}{}_1 = \frac{1 - 1.410\varepsilon_1 + 0.235{\varepsilon_1}^3 + 0.012{\varepsilon_1}^5 + 0.034{\varepsilon_1}^7}{4k^{hk} \cdot l_{die}} \quad (6)$$

$$R^{sp}{}_2 = \frac{1 - 1.410\varepsilon_2 + 0.235{\varepsilon_2}^3 + 0.012{\varepsilon_2}^5 + 0.034{\varepsilon_2}^7}{4k^{hk} \cdot l_{die}} \quad (7)$$

where ε_1 and ε_2 are the ratios of the footprint of the KP chip over that of planar heat sinks at the top and bottom, respectively (*i.e.* $\varepsilon_1 = A_{die}/A^{hk}{}_1$); k^{hk} is the thermal conductivity of the heat sinks; l_{die} is the square root of the footprint of the KP chip ($\sqrt{A_{die}}$). Table 1 lists the parameters and resulting thermal resistances calculated using equations (2)-(7).

Whereas these equations represent one-dimensional approximations, a more accurate representation of the thermal flux was obtained by using COMSOL Multiphysics

Table 1: Parameters in thermal resistance calculations

k_{die}	0.8 Wm^{-1}K^{-1}	k_{MCE}	0.15 Wm^{-1}K^{-1}
A_{die}	256 mm^2	t_{MCE}	500 μm
l_{die}	16 mm	A_{MCE}	256 mm^2
k^{hk}	273 Wm^{-1}K^{-1}	h^{air}	3.43 Wm^{-2}K^{-1}
$t^{die}{}_1$	1 mm	$t^{die}{}_2$	2 mm
$A^{eff}{}_1$	5727 mm^2	$A^{eff}{}_2$	10800 mm^2
ε_1	0.162	ε_2	0.0925
$R^{cd}{}_1$	4.883 KW^{-1}	$R^{cd}{}_2$	22.79 KW^{-1}
$R^{sp}{}_1$	0.051 KW^{-1}	$R^{sp}{}_2$	0.047 KW^{-1}
$R^{cv}{}_1$	50.9 KW^{-1}	$R^{cv}{}_2$	27 KW^{-1}

Table 2: Simulated parameters in COMSOL.

Thermal conductivity ($Wm^{-1}K^{-1}$)			
Aluminum	273	MCE membrane	0.15
Air	0.02	Glass	0.8
Ambient Temperature			25˚C
Heat convection coefficient of air ($Wm^{-2}K^{-1}$)			3.43

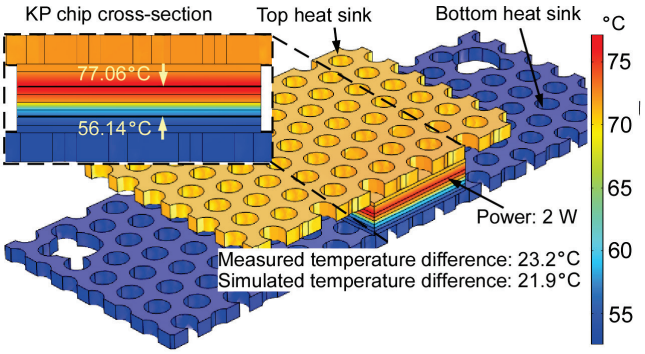

Figure 4: FEA simulation was performed using a custom heat transferring model in COMSOL. The results show the largest temperature difference (ΔT) between the hot and cool sides of the KP is ≈21.9˚C with a power of 2 W.

for finite element analysis (FEA). The main parameters used in the simulation are listed in Table 2. The simulation used approximations for heat sinks to simplify the geometry [12].

Figure 4 shows the estimated temperature difference between the hot side and cool side of the KP. A maximum temperature difference of ≈21.9˚C can be achieved when the KP is powered at ≈2 W. This temperature difference is limited by the maximum operating temperature of MCE membrane of ≈75˚C [13].

RESULTS

The performance of the KP was evaluated using a commercial flow meter (Model # MW-20SCCM-D, Alicat Scientific, Inc., Tuscon, AZ, USA), a differential pressure sensor (MPX5010DP, Freescale Semiconductor Inc., Austin, TX, USA), and a DC power supply, which were interfaced by a custom LabVIEW program (Fig. 5). The flow-rate (Q) and pressure head (ΔP) were recorded with the KP being heated at 0.5 W, 1 W, and 2 W for both pumping directions.

The Q-ΔP relation at each power level was recorded under three different loading conditions – the gas flow path being fully open (with only the flow meter in-line), partially

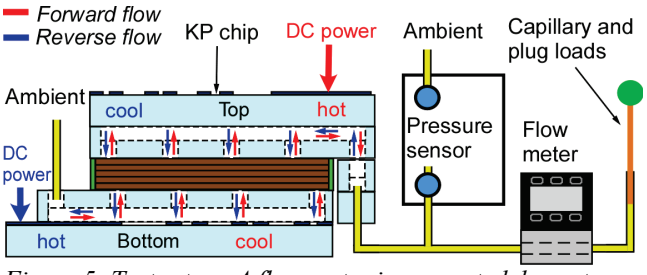

Figure 5: Test setup. A flow meter is connected downstream of the KP. A pressure sensor is used to measure the pressure head between two flow ports of the KP. Extra capillary and plug are used as flow loading.

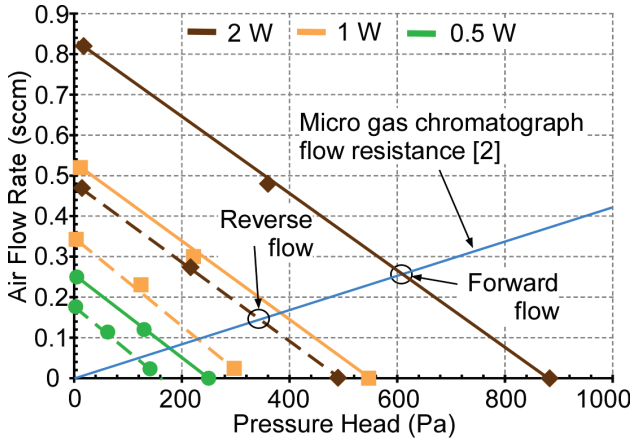

Figure 6: Air flow rate-pressure head relation of the KP. The solid lines and dashed lines represent the performance of the KP in forward and reverse pumping, respectively. The blue line is the flow resistance line of a μGC [4].

blocked, or fully blocked. The loading was made by connecting extra capillary tubes at the end of gas tubing. In experiments, we defined the pumping direction from the bottom side to the top side of the KP chip as forward pumping, and the reverse direction to be reverse pumping.

Measurements confirmed that with higher power applied to the KP, the air flow rate and blocking pressure both increased. At the maximum applied power of 2 W, the KP provided a maximum flow rate of ≈0.82 sccm and a blocking pressure of ≈880 Pa in forward direction, and ≈0.48 sccm and ≈490 Pa in the reverse direction (Fig. 6).

The temperatures on the hot and cool sides of the KP were monitored using the on-chip thermistors. With a power of 2 W, the steady-state temperature difference reached 23.2˚C for forward pumping and 10.1˚C for reverse pumping (Table 3). The measured temperature difference was close to the simulated value, which verified the FEA modeling.

The transient response of the KP was calibrated by measuring the transient change of pressure head in both directions. The transient response (Fig. 7) shows that the flow direction can be switched within 5 minutes.

Table 3: Steady-state temperatures on the hot and cool sides of the KP at different power levels.

Power levels	Temperatures for forward pumping (˚C)			Temperatures for reverse pumping (˚C)		
	T_{hot}	T_{cool}	ΔT	T_{hot}	T_{cool}	ΔT
0.5 W	33.7	27.1	6.6	27.3	24.4	2.9
1 W	46.4	32.2	14.2	33.8	27.9	5.9
2 W	65.7	42.5	23.2	62	51.9	10.1

DISCUSSION AND CONCLUSION

The steady-state bidirectional performance of the KP was compared to previous reports with consideration for flow rate, pressure head, and power consumption. To enable fair comparison of different KPs operating at different power levels, the bidirectional performance was calculated as:

$$\bar{Q} \cdot \Delta\bar{P}_{eq} / \bar{W}_P{}^2 \qquad (9)$$

where $\bar{Q}$ is the average flow rate in both directions, $\Delta\bar{P}_{eq}$ is

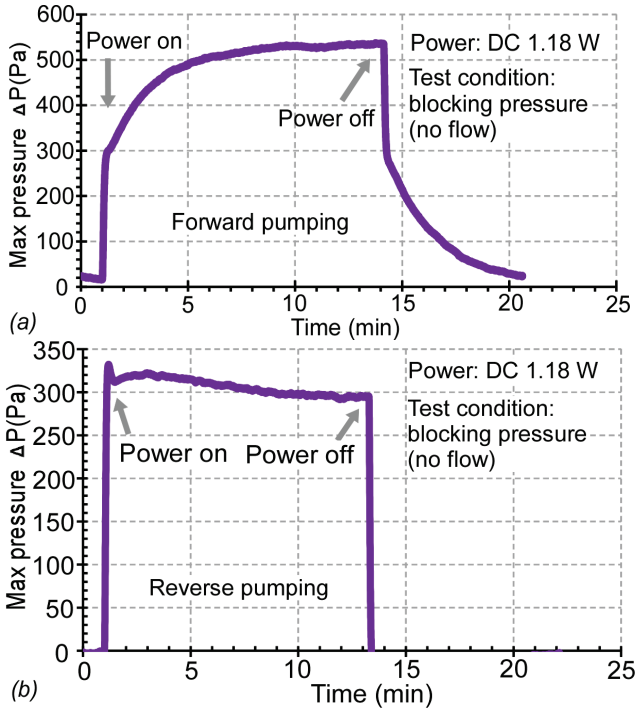

Figure 7: Transient response of the KP for (a) forward pumping, and (b) reverse pumping.

the average blocking pressure head in both directions, and $\bar{W}_P$ is average power applied in both directions for the maximum performance. This KP provided a bidirectional performance of ≈111.3 sccm·Pa/W^2. This result presents 2X-3X improvement over prior reports (Fig. 8).

Overall, this work demonstrates a bidirectional Knudsen pump architecture that integrates a micromachined chip with customized heat sinks as a whole solution. Superior thermal management is achieved on both sides of the KP to permit effective pumping in both directions. The heat sinks, which are thin, planar, and perforated, can effectively dissipate heat from the KP to the ambient. As a consequence, a large temperature difference (≈23.2˚C) can be established between the hot and cool sides of the KP with modest power consumption (2 W). Further, this leads to an improvement in the performance of the bidirectional KP by 2X-3X compared

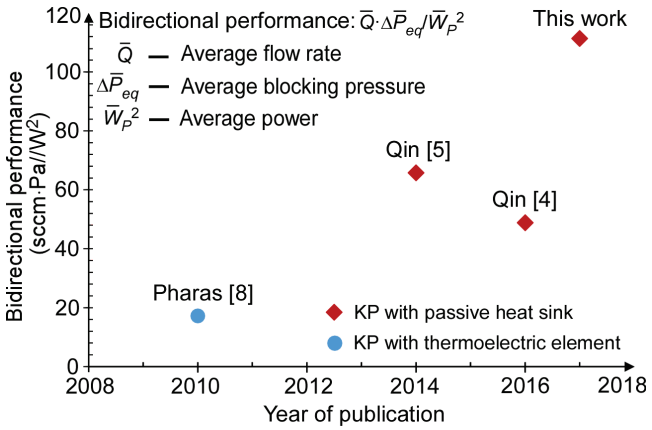

Figure 8: Performance of the bidirectional KP is improved by 2X-3X compared to prior work.

to the previous reports. If connected to a typical μGC [4], this KP could provide ≈0.25 sccm for separation and ≈0.15 sccm for sampling, which would be sufficient for proper system operation.

The entire KP architecture is reliable, silent, and compact. All these features make the KP attractive for many portable systems requiring bidirectional flow.

ACKNOWLEDGEMENTS

This effort was supported by the University of Michigan.

REFERENCES

[1] T.M. Squires, S.R. Quake, "Microfluidics: Fluid physics at the nanoliter scale," *Reviews of Modern Physics*, vol. 77, pp. 977–1026, 2005.

[2] R.R.A. Syms, S. Wright, "MEMS mass spectrometers: the next wave of miniaturization," *J. Micromechanics & Microengineering*., vol. 26, pp. 023001, 2016.

[3] C.J. Lu, *et al.*, "First-generation hybrid MEMS gas chromatograph", *Lab on a Chip*, vol. 5, pp. 1123., 2005

[4] Y. Qin, Y.B. Gianchandani, "A fully electronic microfabricated gas chromatograph with complementary capacitive detectors for indoor pollutants," *Nature Microsystems & Nanoeng.*, vol. 2, pp. 15046, 2016.

[5] Y. Qin, Y.B. Gianchandani, "iGC2: An architecture for micro gas chromatographs utilizing integrated bi-directional pumps and multi-stage preconcentrators," *J. Micromech. & Microeng*., vol. 24, pp. 10, 2014.

[6] M. Knudsen, "Die Molekularströmung der Gase durch Offnungen und die Effusion," *Annalen der Physik, Leipzig,* 336(1), pp. 205-229., 1909.

[7] N.K. Gupta, Y.B. Gianchandani, "Thermal transpiration in mixed cellulose ester membranes: enabling miniature, motionless gas pumps," *Microporous Mesoporous Mater.*, vol. 142, pp. 535–41, 2011.

[8] K. Pharas and S. McNamara, "Knudsen pump driven by a thermoelectric material," *J. Micromech. & Microeng.*, vol. 20, pp. 12, 2010.

[9] F. Sharipov, "Rarefied gas flow through a long tube at arbitrary pressure and temperature drops," *J. Vacuum. Sci. Technol. A.* vol. 15, pp. 2434, 1997.

[10] J.H. Lienhard IV, J.H. Lienhard V, *A Heat Transfer Textbook: Fourth Edition*, Corier Corporation, 2011

[11] M.M. Yovanovich, E.E. Marotta, *Heat Transfer Handbook (Chapter 4)*, John Wiley and Sons Inc., 2003

[12] Z. Staliulionis, *et al.*, "Investigation of heat sink efficiency for electronic component cooling applications," *Elektronika ir Elektrotechnika*. vol. 20, pp.1, 2014.

[13] MilliporeSigma Inc., "Specification sheet of MF-Milipore MCE membrane filters," [Online]. [Accessed: 17-Nov-2016].

CONTACT

*Q. Cheng, email: qisench@umich.edu
*Y. Qin: yutaoqin@umich.edu
*Y.B. Gianchandani: yogesh@umich.edu